Counterion-Induced Reversibly Switchable Transparency in Smart Windows

Chang Hwan Lee,[†,§] Ho Sun Lim,[‡,§,*] Jooyong Kim,[†,*] and Jeong Ho Cho[†,*]

[†]Department of Organic Materials and Fiber Engineering, Soongsil University, Seoul 156-743, Republic of Korea, and [‡]Electronic Materials and Device Research Center, Korea Electronics Technology Institute, Gyeonggi-do 463-816, Republic of Korea. [§]These authors contributed equally to this work.

ABSTRACT Smart windows that can reversibly alternate between extreme optical characteristics *via* clicking counteranions of different hydration energies were developed on glass substrates through the facile spray-casting of poly[2-(methacryloyloxy)ethyltrimethylammonium chloride-*co*-3-(trimethoxysilyl)propyl methacrylate]. The optical transmittance was either 90.9% or 0% over the whole spectral range when alternately immersed in solutions containing thiocyanate (SCN^-) or bis(trifluoromethane)sulfonimide ($TFSI^-$) ions, respectively. The extreme optical transitions were attributed to formation of microporous structures *via* the molecular aggregation of polyelectrolyte chains bearing $TFSI^-$ ions in methanol. Because the smart windows were either highly transparent toward or completely blocking of incident light upon direct counterion exchange, this kind of nanotechnology may provide a new platform for efficiently conserving on energy usage in the interior of buildings.

KEYWORDS: polyelectrolytes · tunable transparency · smart windows · ion exchange · functionality · saving on energy

One of the most important issues of the 21st century is the looming fact that the world will be faced with a serious scarcity of energy.[1,2] To address the fast-approaching energy crisis, the past decade has seen a large number of research efforts that have struggled to develop renewable energy sources from natural resources, such as sunlight, wind, rain, tides, biomass, and geothermal heat.[1,2] Moreover, current interest has been concentrated on ways to effectively use our finite energy resources by improving energy efficiency, operating at lower rates of energy consumption, storing energy, and conserving energy.[3−5] Recently, in this context, smart windows, which can tailor light transmittance in response to environmental circumstance, are particularly intriguing as a potential alternative to economizing on energy.[6−14] They can lead to practical applications, such as house roofs, skylights, architectural or vehicle windows, and interior partitions. Since smart windows can appropriately modulate heat transfer from the transmitted sunlight in a house, they can moderately suppress unnecessary energy usage through air conditioning or heating. For example, smart windows can prevent the inside of a building from becoming overheated by reflecting away a large fraction of the incident sunlight in summer. Alternatively, they can help keep a room warm by absorbing the sun's heat in winter. In principal, optical switching of smart windows has been achieved to control light propagation or absorption either by aligning liquid crystals, by dispersing suspended particles, or by stimulating the oxidation−reduction transduction of chromophores in response to light irradiation, electric charge, or temperature changes.[8−10] However, until now, the numerous technologies developed not only have been chemically unstable, prohibiting their use in long-term switching applications but have been accompanied by the use of expensive special equipment and complicated harsh processing conditions.

In this study, we have developed a novel smart window system with extremely tunable transparency, which conveys either the high transmittance ($T \approx 90.9\%$) or complete blockage ($T \approx 0\%$) of incident light *via* direct counterion exchange. To our knowledge, such extreme optical switching behavior is unprecedented among established smart windows. We have employed polyelectrolytes with quaternary ammonium (QA^+) groups as a building block, paying particular attention to their aggregation and conformational changes at the nanoscale as a function of the hydration properties of the diversified counteranions.[15,16] Polyelectrolytes composed of hydrophobic nonionic segments and hydrophilic ionic segments, mounted on substrates, induce reversible morphological changes due to molecular reorganization as a function of polymer chain solvation by appropriate selection of the counteranion.[17,18] An interesting

* Address correspondence to
hslim@keti.re.kr,
jykim@ssu.ac.kr,
jhcho94@ssu.ac.kr.

Received for review June 23, 2011
and accepted August 5, 2011.

10.1021/nn202328y

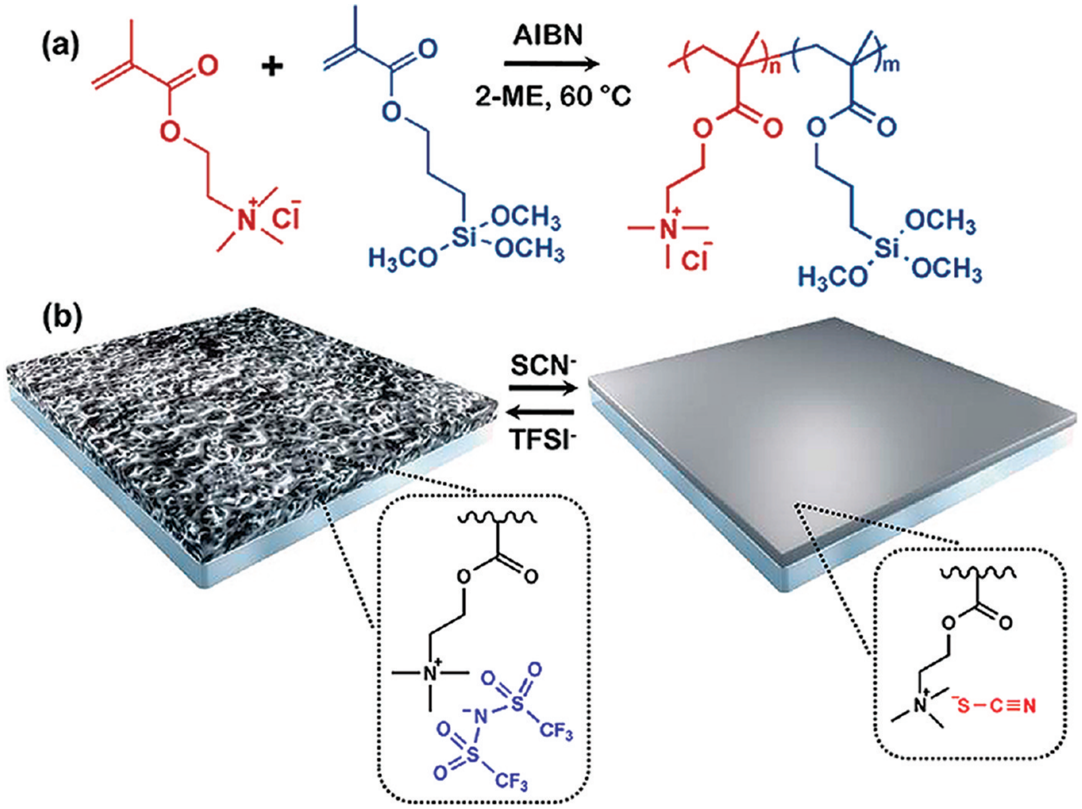

Figure 1. (a) Reaction scheme for the polymerization of poly(METAC-*co*-TSPM). (b) Schematic representation for the reversible morphological changes of poly(METAC-*co*-TSPM)-coated smart windows with switchable optical transmittance as a result of direct counterion exchange.

property of polyelectrolytes is that their solvophobicity (hydrophobicity) and solvophilicity (hydrophilicity) can be easily tuned by exchanging the counterions. Therefore, the surface architecture may be facilely adjusted by specific organic solvents (or water), leading to the extremely reversible optical switching from transparent to opaque states *via* counterion-induced molecular aggregation of polyelectrolyte brushes at the nanoscale.

RESULTS AND DISCUSSION

To produce smart windows with extremely tunable light transmittance, we synthesized poly[2-(methacryloyloxy)ethyltrimethylammonium chloride-*co*-3-(trimethoxysilyl)propyl methacrylate] (poly(METAC-*co*-TSPM)) as a cross-linkable polyelectrolyte copolymer *via* free radical copolymerization (Figure 1a).[19] PolyMETAC was selected as the polyelectrolyte for the molecular aggregation and reorganization of the polymer chains in response to organic solvents as a result of ion exchange, and TSPM was adopted as a sol−gel precursor not only to anchor the polyelectrolytes on the substrates but also to form a polymer network due to inter- or intramolecular cross-linking between polymer chains. The resulting polymers were dissolved in aqueous methanol, followed by spray-casting to form optically clear films several micrometers thick on glass substrates.[20] As expected, the transmittance of the as-prepared glass, which coordinated with Cl^- anions as counterions, was ∼91.3% over a broad range of wavelengths due to its uniformly smooth surface morphology. It was highly transparent to the naked eye. In particular, the functionalized glass remained decidedly limpid even in the near-IR region.

Reversible optical switching of smart windows was facilely achieved by exchanging counteranions selected from a diverse array of hydration energies (Movie S1). Upon soaking in a methanol solution containing 2.5 mM lithium bis(trifluoromethane) sulfonimide salt, the coordinated Cl^- ions that permeated the polymer gels were progressively replaced with bis(trifluoromethane)sulfonimide ($TFSI^-$) ions. The poly(METAC-*co*-TSPM) grafted glass lost its optical transparency (Figure 2a). This result was attributed to the immense scattering of incident light off of surface nanostructures.[21] In contrast with the polyelectrolytes-grafted film coordinated to $TFSI^-$ ions, once the opaque glass sheet was immersed in a 2.5 mM sodium thiocyanate salt solution, the poly(METAC-*co*-TSPM)-modified glass substrate became gradually pellucid, and its transmittance reached 90.9% over a wide bandwidth spanning the ultraviolet−visible−near IR spectrum (Figure 2b). The poly(METAC-*co*-TSPM) polyelectrolytes combined with the thiocyanate (SCN^-) ions

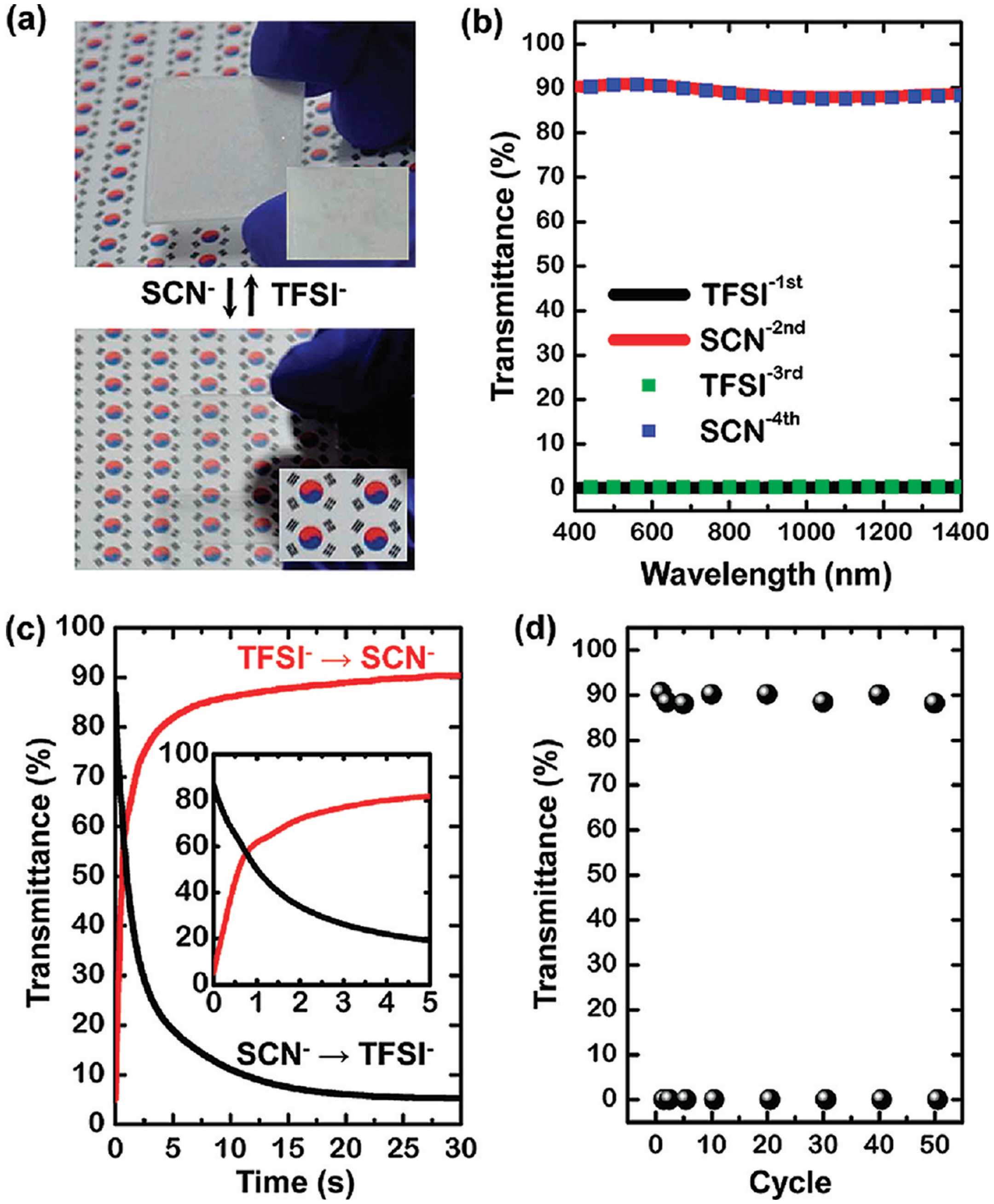

Figure 2. (a) Optical images of the poly(METAC-*co*-TSPM)-deposited glass overlaying a printed paper. The reversible switching of transmittance from opaque (upper) to transparent (lower) corresponded to ion exchange from TFSI$^-$ to SCN$^-$ ions. (b) Transmittance spectra of the glass substrates at normal incident light *via* direct ion exchange. (c) Time-dependent changes in optical transmittance of the glass films as a function of ion exchange between TFSI$^-$ and SCN$^-$ ions. The inset shows the magnified transmittance spectra in the initial stage. (d) Reversible optical switching of the glass sheets at 550 nm during 50 cycles as a result of ion exchange.

dissolved well in methanol, resulting in featureless uniform surface structures.

The observed extremely tunable optical behavior may be explained by the phase separation of the poly(METAC-*co*-TSPM) polymers coordinated with TFSI$^-$ ions in methanol as a result of ion exchange (Figure 1b).[22] In principal, the molecular conformation of a polyelectrolyte chain in solvent depends on the balance of repulsive Coulomb and attractive solvophobic interactions.[23−25] As shown in Figure 3a, optical microscopy (OM) images provided evidence that the surface morphology presented hierarchical microporous network structures. Scanning electron microscopy (SEM) images also displayed several micropores 5−10 μm in diameter on the topmost surface, in agreement with the results from OM images. Atomic force microscopy (AFM) images showed that the window films with SCN$^-$ ions exhibited completely even surface morphologies, whereas the glass sheet bearing TFSI$^-$ ions presented roughened surfaces due to nanostructures

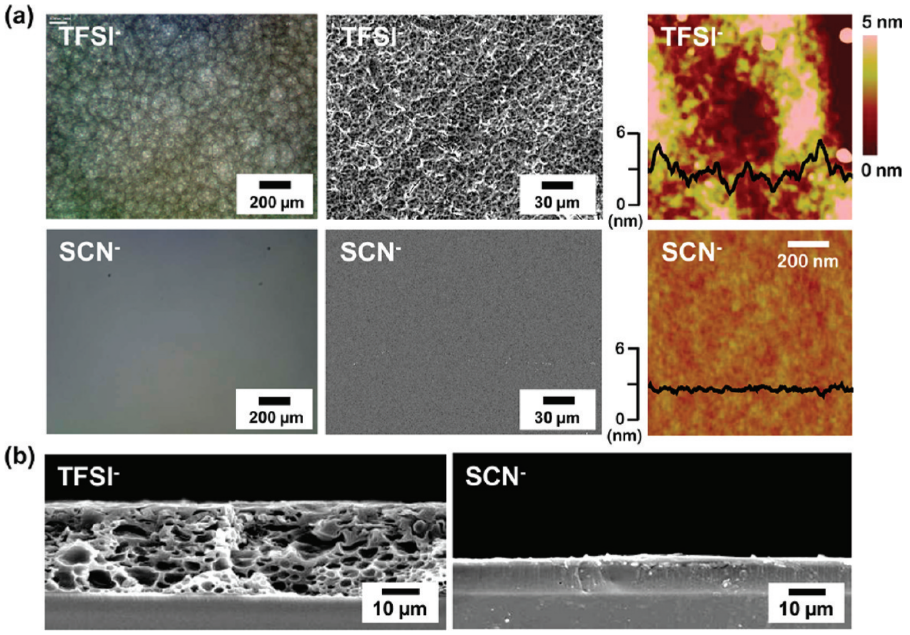

Figure 3. Morphological changes of the poly(METAC-*co*-TSPM)-coated glass films with ion exchange. (a) Optical microscopy (OM), scanning electron microscopy (SEM), and tapping mode atomic force microscopy (AFM) height images of the glass surfaces with TFSI$^-$ (upper) and SCN$^-$ (lower) ions, respectively. (b) Cross-sectional SEM images of the glass sheets coordinated to TFSI$^-$ (left) and SCN$^-$ (right) ions, respectively.

resulting from the molecular aggregation of polyelectrolytes. The peak-to-peak height, which is the height difference between the highest and lowest pixels, increased from almost zero for SCN$^-$ ions to ~4.5 nm for TFSI$^-$ ions, as shown in the height profile AFM images. This means that the microporous structures of the smart windows originated in the molecular aggregation of polymer chains at the nanoscale. Figure 3b shows cross-sectional images of the polyelectrolytes-deposited film, in which the inner structures were composed of a hierarchically interconnected porous network on the substrate. Several pores formed by the phase separation of the polyelectrolytes are clearly visible on the internal structures of the glass sheet. The film thickness expanded by a factor of 2.5 to accommodate the SCN$^-$ ions due to the sponge-like structure generated by the phase separation and molecular aggregation of polymers. This is presumably due to the fact that the polyelectrolytes-grafted film containing TFSI$^-$ ions have poor solubility in methanol, so that phase separation in the thin polymer films tends to result in porous net-like nanostructures with isolated micrometer-sized pores. Consequently, the specific interactions between the poly(METAC-*co*-TSPM) and solvent are altered by the different counteranions, which influences the molecular aggregation of polyelectrolytes, allowing smart windows to display extremely tunable optical properties. The use of the counterions with similar hydration properties would exhibit an analogous optical behavior in transmittance, resulting from a control of a phase separation of polymer chains.

The management of light propagation through these morphological changes originated at the nanoscale over the entire visible spectrum gives rise to the basic concept of developing smart windows with extreme optical switching capabilities that can obediently block or allow heat transfer from transmitted sunlight into a room. When the poly(METAC-*co*-TSPM) polyelectrolytes were coordinated with TFSI$^-$ ions, scattering by the microporous surface textures reflected almost 100% of the incident light, whereas substitution with SCN$^-$ ions made the window extensively transparent over the spectrum from 350 to 1400 nm (Figure 2b). The smart windows demonstrated absorption capabilities exceeding 90% of the available sunlight.

We have also investigated the dynamics of the ion exchange behavior through *in situ* measurements of the UV–vis transmittance when the counteranions coordinated to the polyelectrolytes were exchanged between TFSI$^-$ and SCN$^-$ ions, or *vice versa* (Figure 2c). The thickness of the dry film was about 10 μm, as shown in Figure 3b. It was found that the time required to transition from coordination with TFSI$^-$ to coordination with SCN$^-$ ions was faster than the reverse reaction. As TFSI$^-$ ions were substituted with SCN$^-$ ions, the optical transmittance at 550 nm increased dramatically by up to 80% within 1.25 s of the exchange, followed by slow saturation to 90.3%. However, since the glass film was sufficiently transparent to the human eye, even at 80% transmittance, it took less than 2 s to substantially finish the ion exchange process. In contrast, the optical properties suddenly worsened upon replacing SCN$^-$ with TFSI$^-$ ions, but at least 2.16 s were required to reach 30% transmittance, which marked the change from a transparent to an opaque state. This difference in transition times may be

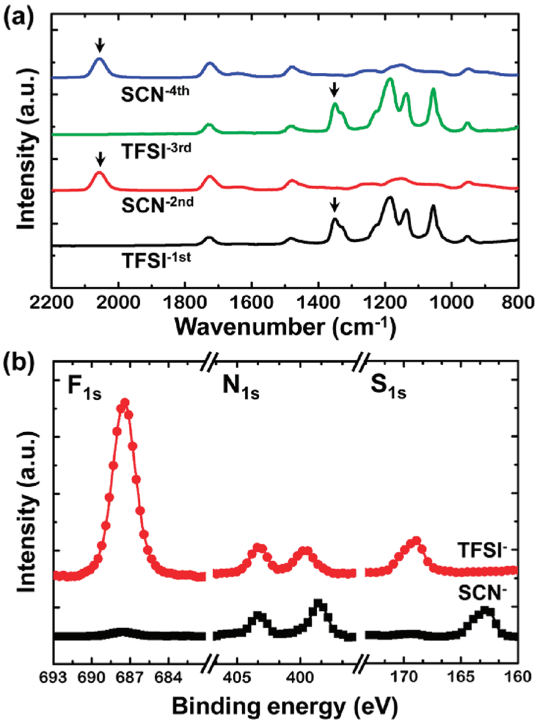

Figure 4. (a) FT-IR and (b) XPS spectra of the poly(METAC-*co*-TSPM)-coated glass substrates *via* direct ion exchange from TFSI$^-$ to SCN$^-$ ions.

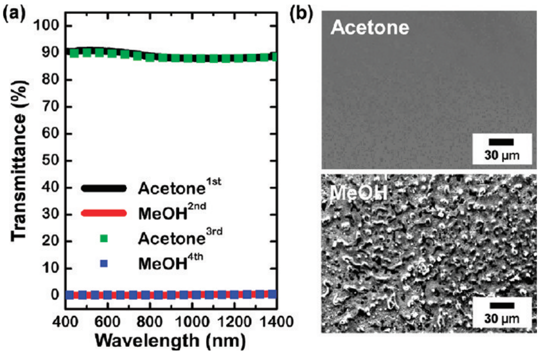

Figure 5. (a) Transmittance spectra of the poly(METAC-*co*-TSPM)-modified glass substrates coordinated to TFSI$^-$ ions at normal incident light upon solvent exchange. (b) SEM images of the glass sheet immersed in acetone (upper) and methanol (lower), respectively.

attributed to the fact that the surface morphology formed in the presence of TFSI$^-$ ions consisted of three-dimensional micro/nanoporous structures, whereas that formed upon coordination of SCN$^-$ ions was smooth, as shown in Figure 3a. Thus, the surface area that contacted the solutions was larger when enclosing TFSI$^-$ ions than when containing SCN$^-$ ions. The smooth SCN$^-$-coordinated surface significantly lengthened the required time for ion exchange. In addition, the changes in the optical transmittance were reversible without incurring significant damages even after 50 exchange cycles (Figure 2d). This smart window still exhibited extreme transmittance variations from 90.2% for SCN$^-$ ions to almost 0% for TFSI$^-$ ions.

The successful ion exchange behavior of the poly(METAC-*co*-TSPM) brush-modified glass substrates was observed by measuring the FT-IR spectra (Figure 4a).[16] The existence of TFSI$^-$ ions in the poly(METAC-*co*-TSPM) brushes was confirmed by the appearance of a new signal at 1356 cm^{-1}, which corresponded to the stretching vibration of the CF$_3$ groups. Once the TFSI$^-$ ions were substituted with SCN$^-$ ions, the peak at 1356 cm^{-1} disappeared and a new absorption peak appeared at 2082 cm^{-1}, assigned to the SCN groups. The reversible IR spectral changes indicate that the ion exchange reaction successfully occurs upon soaking in solutions with different counteranions. Similarly, the F 1s, C 1s, and N 1s peaks of the poly(METAC-*co*-TSPM)-coated glass were evaluated by XPS measurements as a function of ion exchange (Figure 4b).[26] The F 1s spectra could be fit only to a single peak at a binding energy of 687.5 eV, indicating the presence of fluorine atoms; that is, the Cl$^-$ ions in the polymer brushes were completely replaced with TFSI$^-$ ions. The N 1s peak of the glass substrates, after exchange of the TFSI$^-$ ions, could be fit to two peak components, at 399.7 and 403.3 eV, attributed to the neutral nitrogen atoms in the TFSI$^-$ ions and to the positively charged nitrogen atoms in the QA$^+$ groups, respectively. These results indicate that the Cl$^-$-coordinated polyelectrolyte gels were successfully converted into TFSI$^-$-coordinated gels. After the subsequent ion exchange with SCN$^-$ ions, the F 1s peak at 687.5 eV and the S 2*p* peak at 169.0 eV, assigned to the sulfonyl groups of the TFSI$^-$ ion, disappeared and a new S 2*p* peak at a binding energy of 163.2 eV, corresponding to the SCN$^-$ ions, appeared, corroborating the subtraction of TFSI$^-$ ions and the introduction of SCN$^-$ ions. Moreover, coordination of the poly(METAC-*co*-TSPM) to TFSI$^-$ ions created a hydrophobic surface due to the fluorine atoms in the coordinated counteranion. The water contact angle (CA) for this surface was 90 ± 2°, and the surface was smooth. Replacing TFSI$^-$ with the slightly hydrophilic SCN$^-$ ions altered the water CA to 65 ± 1°. The wettability of the poly(METAC-*co*-TSPM)-anchored smooth surface changed reversibly depending on the hydration properties of the TFSI$^-$ and SCN$^-$ ions.[18] These results indicate that extreme optical switching in the smart windows originates from the swapping of counteranions, which can be reversibly exchanged with other anions of different hydration energies without damaging the polyelectrolyte film.

Moreover, we found that immersion in acetone increased the transmittance of the poly(METAC-*co*-TSPM)-coated glass slides bearing TFSI$^-$ ions by almost 90.1%, implying solubility-driven optical tunability of the smart windows *via* solvent exchange (Figure 5). Although the polyelectrolytes remained coordinated to the TFSI$^-$ ions, they tended to be highly transparent to the human eye, similar to the films coordinated with

SCN⁻ ions in methanol. The phase separation-induced surface morphology was strongly affected by not only the solubility of the polymers but also the evaporation rate of the solvent. When the poly(METAC-*co*-TSPM)-deposited glass sheet with TFSI⁻ ions was contacted with 2-methoxyethanol, the sheet appeared hazy and translucent because the surface was covered with ruggedly embossed nanoprotuberances due to the slow and irregular volatilization of 2-methoxyethanol across the surface (Figure S2). However, soaking the glass slide in acetone produced featureless surface structures, because acetone tended not only to dissolve well the polyelectrolytes coordinated to TFSI⁻ ions but also to rapidly escape as vapor from the top surface layer. Furthermore, immersion in ethyl acetate, which features a relatively low vapor pressure, produced a transparency that was similar to that produced in acetone. These results indicate that the use of a rapidly volatile, good solvent makes the smart windows optically transparent, and *vice versa*.

CONCLUSION

We describe functional smart windows that exhibit reversibly switchable optical characteristics by converting between strongly opaque and highly transparent states upon exchange of counteranions with different hydration energies. The unprecedented extreme optical transitions were achieved by formation of microporous structures attributed to the nanophase separation of polyelectrolytes. We consider two switches for the manipulation of light propagation in smart windows: (i) direct exchange of counterions with diversified hydration energies and (ii) control of the solvophobicity in polymers. This type of light control system may provide a new option for saving on heating, cooling, and lighting costs through managing the light transmitted into the interior of a house. The windows may be applied in a wide range of fields such as roof tiles, automobiles, and architectural windows.

METHODS

Sample Preparation. Poly[2-(methacryloyloxy)ethyltrimethylammonium chloride-*co*-3-(trimethoxysilyl)propyl methacrylate] (poly(METAC-*co*-TSPM)) as an alkoxysilane-cross-linkable polyelectrolyte copolymer was synthesized through conventional free radical copolymerization. All reagents and starting materials were purchased from Aldrich Chemical Inc. 2-(Methacryloyloxy)ethyltrimethylammonium chloride (METAC) was purified on an alumina column after the evaporation of water, and 3-(trimethoxysilyl)propyl methacrylate (TSPM) was used without further purification. α,α'-Azobisisobutyronitrile (AIBN) was recrystallized from methanol. A mixture of METAC (16.56 g, 80 mmol), TSPM (4.96 g, 20 mmol), and AIBN (0.16 g, 0.1 mmol) dissolved in anhydrous 2-methoxyethanol (150 g) was placed in a round-bottom flask. The feed ratio of METAC, TSPM, and AIBN was 800:200:1. The solution was degassed by the freeze−thaw method, repeated three times. The sealed reaction bottle was heated at 60 °C and maintained for 12 h. The polymerized mixture was precipitated twice in a large volume of THF, then vacuum-filtered. The solid powdery product was freeze-dried for 24 h under vacuum, then stored in a desiccator. The copolymer contained TSPM monomers of 22 mol % (Figure S1). The resulting polymers were dissolved in 80 wt % aqueous methanol and then spray-cast to several micrometer thickness onto clean glass substrates.

Characterization. The film morphologies were imaged by optical microscopy (SOMTECH I-MEGASCOPE), scanning electron microscopy (JEOL JSM-6360), and atomic force microscopy (Digital Instrument Nanoscope IIIa). Fourier transform infrared (FT-IR) spectra were recorded on an FTIR-6300 (JASCO) spectrometer in transmittance mode with a resolution of 4 cm^{-1}. Optical transmittance of glass was measured as functions of wavelength with a UV−vis−NIR spectrophotometer (JASCO V-670 spectrometer). Dynamic ion exchanging behavior was characterized with a Shimadzu UV-3600. X-ray photoelectron spectroscopy was performed at the 4B1 beamline at the Pohang Accelerator Laboratory.

Acknowledgment. This study was supported by the Energy & Resource Development Program (2010T100200201) of the Ministry of Knowledge Economy (MKE) and the National Research Foundation of Korea (NRF) funded by the Ministry of Education, Science and Technology (2010-0003941), Korea.

Supporting Information Available: Additional characterization data. This material is available free of charge *via* the Internet at http://pubs.acs.org.

REFERENCES AND NOTES

1. Fanchi, J. R. *Energy in the 21st Century*; World Scientific: Hackensack, N.J., 2005.
2. Nersesian, R. L. *Energy for the 21st Century: A Comprehensive Guide to Conventional and Alternative Sources*; M.E. Sharpe: Armonk, N.Y., 2007.
3. Dresselhaus, M. S.; Dresselhaus, G.; Charlier, J. C.; Hernandez, E. Electronic, Thermal and Mechanical Properties of Carbon Nanotubes. *Philos. Trans. R. Soc., A* **2004**, *362*, 2065–2098.
4. Girishkumar, G.; McCloskey, B.; Luntz, A. C.; Swanson, S.; Wilcke, W. Lithium-Air Battery: Promise and Challenges. *J. Phys. Chem. Lett.* **2010**, *1*, 2193–2203.
5. Ulbricht, R.; Lee, S. B.; Jiang, X. M.; Inoue, K.; Zhang, M.; Fang, S. L.; Baughman, R. H.; Zakhidov, A. A. Transparent Carbon Nanotube Sheets as 3-D Charge Collectors in Organic Solar Cells. *Sol. Energy Mater. Sol. Cells* **2007**, *91*, 416–419.
6. Debije, M. G. Solar Energy Collectors with Tunable Transmission. *Adv. Funct. Mater.* **2010**, *20*, 1498–1502.
7. Baetens, R.; Jelle, B. P.; Gustavsen, A. Properties, Requirements and Possibilities of Smart Windows for Dynamic Daylight and Solar Energy Control in Buildings: A State-of-the-Art Review. *Sol. Energy Mater. Sol. Cells* **2010**, *94*, 87–105.
8. Bechinger, C.; Ferrer, S.; Zaban, A.; Sprague, J.; Gregg, B. A. Photoelectrochromic Windows and Displays. *Nature* **1996**, *383*, 608–610.
9. Beaujuge, P. M.; Ellinger, S.; Reynolds, J. R. The Donor-Acceptor Approach Allows a Black-to-Transmissive Switching Polymeric Electrochrome. *Nat. Mater.* **2008**, *7*, 795–799.
10. Cupelli, D.; Nicoletta, F. P.; Manfredi, S.; Vivacqua, M.; Formoso, P.; De Filpo, G.; Chidichimo, G. Self-Adjusting Smart Windows Based on Polymer-Dispersed Liquid Crystals. *Sol. Energy Mater. Sol. Cells* **2009**, *93*, 2008–2012.
11. Lanzo, J.; De Benedittis, M.; De Simone, B. C.; Imbardelli, D.; Formoso, P.; Manfredi, S.; Chidichimo, G. Photoelectrochromic Switchable Nematic Emulsions. *J. Mater. Chem.* **2007**, *17*, 1412–1415.

12. Nicoletta, F. P.; Chidichimo, G.; Cupelli, D.; De Filpo, G.; De Benedittis, M.; Gabriele, B.; Salerno, G.; Fazio, A. Electrochromic Polymer-Dispersed Liquid-Crystal Film: A New Bifunctional Device. *Adv. Funct. Mater.* **2005**, *15*, 995–999.
13. Beaujuge, P. M.; Reynolds, J. R. Color Control in π-Conjugated Organic Polymers for Use in Electrochromic Devices. *Chem. Rev.* **2010**, *110*, 268–320.
14. Cupelli, D.; De Filpo, G.; Chidichimo, G.; Nicoletta, F. P. The Electro-Optical and Electrochromic Properties of Electrolyte-Liquid Crystal Dispersions. *J. Appl. Phys.* **2006**, *100*, 024515.
15. Moya, S.; Azzaroni, O.; Farhan, T.; Osborne, V. L.; Huck, W. T. S. Locking and Unlocking of Polyelectrolyte Brushes: Toward the Fabrication of Chemically Controlled Nanoactuators. *Angew. Chem., Int. Ed.* **2005**, *44*, 4578–4581.
16. Azzaroni, O.; Moya, S.; Farhan, T.; Brown, A. A.; Huck, W. T. S. Switching the Properties of Polyelectrolyte Brushes via "Hydrophobic Collapse". *Macromolecules* **2005**, *38*, 10192–10199.
17. Azzaroni, O.; Brown, A. A.; Huck, W. T. S. Tunable Wettability by Clicking Counterions into Polyelectrolyte Brushes. *Adv. Mater.* **2007**, *19*, 151–154.
18. Lim, H. S.; Lee, S. G.; Lee, D. H.; Lee, D. Y.; Lee, S.; Cho, K. Superhydrophobic to Superhydrophilic Wetting Transition with Programmable Ion-Pairing Interaction. *Adv. Mater.* **2008**, *20*, 4438–4441.
19. Lee, C. W.; Choi, B. K.; Gong, M. S. Humidity Sensitive Properties of Alkoxysilane-Crosslinked Polyelectrolyte Using Sol-Gel Process. *Analyst* **2004**, *129*, 651–656.
20. Amb, C. M.; Beaujuge, P. M.; Reynolds, J. R. Spray-Processable Blue-to-Highly Transmissive Switching Polymer Electrochromes via the Donor−Acceptor Approach. *Adv. Mater.* **2010**, *22*, 724–728.
21. Mie, G. Contributions to the Optics of Turbid Media, Especially Colloidal Metal Solutions. *Ann. Phys.-Berlin* **1908**, *25*, 377–445.
22. Tokarev, I.; Minko, S. Stimuli-Responsive Porous Hydrogels at Interfaces for Molecular Filtration, Separation, Controlled Release, and Gating in Capsules and Membranes. *Adv. Mater.* **2010**, *22*, 3446–3462.
23. Dobrynin, A. V. Electrostatic Persistence Length of Semiflexible and Flexible Polyelectrolytes. *Macromolecules* **2005**, *38*, 9304–9314.
24. Holm, C.; Joanny, J. F.; Kremer, K.; Netz, R. R.; Reineker, P.; Seidel, C.; Vilgis, T. A.; Winkler, R. G. Polyelectrolyte Theory. *Adv. Polym. Sci.* **2004**, *166*, 67–111.
25. Dobrynin, A. V.; Rubinstein, M. Theory of Polyelectrolytes in Solutions and at Surfaces. *Prog. Polym. Sci.* **2005**, *30*, 1049–1118.
26. Bomben, K. D.; Moulder, J. F.; Sobol, P. E.; Stickle, W. F. *Handbook of X-ray Photoelectron Spectroscopy. A Reference Book of Standard Spectra for Identification and Interpretation of XPS Data*; Physical Electronics: Eden Prairie, MN, 1995.